# Effects of Air Void at the Steel-Concrete Interface on the Corrosion Initiation of Reinforcing Steel in Concrete under Chloride Exposure

Jin-Gak Nam[1], William H. Hartt[1], and Kijoon Kim[2]*

[1] Florida Atlantic University, Florida, USA
[2] Korea Maritime University, Busan, 606-791, Korea

## Abstract

A series of reinforced G109 type specimens was fabricated and ponded with a 15 weight percent NaCl solution. Mix design variables included 1) two cement alkalinities (equivalent alkalinities of 0.32 and 1.08), 2) w/c 0.50 and 3) two rebar surface conditions (as-received and wire-brushed). Potential and macro-cell current between top and bottom bars were monitored to determine corrosion initiation time. Once corrosion was initiated, the specimen was ultimately autopsied to perform visual inspection, and the procedure included determination of the number and size of air voids along the top half of the upper steel surface. This size determination was based upon a diameter measurement assuming the air voids to be half spheres or ellipse. The followings were reached based upon the visual inspection of G109 specimens that were autopsied to date. First, voids at the steel-concrete interface facilitated passive film breakdown and onset of localized corrosion. Based upon this, the initiation mechanism probably involved a concentration cell with contiguous concrete coated and bare steel serving as cathodes and anodes, respectively. Second, the corrosion tended to initiate at relatively large voids. Third, specimens with wire-brushed steel had a lower number of voids at the interface for both cement alkalinities, suggesting that air voids preferentially formed on the rough as-received surface compared to the smooth wire brushed one.

Keywords: air void, cement alkalinity, steel-concrete interface, passive film, cathode

## 1. Introduction

It has been recognized for more than a century that concrete comprised of Portland cement affords corrosion protection to embedded steel. The protective mechanism is mostly due to a thin passive film of $\gamma$-$Fe_2O_3$ that is formed and maintained upon the steel in the alkaline environment produced by cement hydration.[1] However, the passive layer can be compromised when even modest concentrations of chlorides are present at the steel-concrete interface, leading to active corrosion followed by concrete cracking and spalling.

Solutions that intend to simulate concrete pore water have been widely used in corrosion studies; however, for reasons that are not completely understood, reinforcing steel is generally more resistant to corrosion in actual concrete than in such solutions.[2] One possible explanation is

presence of a dense cement rich layer containing significant quantities of $Ca(OH)_2$ at the steel concrete interface. This layer serves as a source of hydroxide ions which counters any pH drop that occurs in conjunction with pit initiation or carbonation.[3]

Yonezawa et al.[4] reported that good physical adhesion between iron oxides on the steel surface and cement hydrates is an important aspect of achieving good corrosion resistance. In addition, these authors concluded that the formation of voids at the steel-concrete interface was "essential" for corrosion initiation. This is consistent with the findings of Monfore and Verbeck[5] who had previously reported that corrosion of prestressing steel was associated with air voids at the steel-concrete interface. More recently, Glass and Reddy[6] used low magnification microscopy and image analysis to measure void area at the steel-concrete interface. They reported that the chloride threshold depended on entrapped air voids. Also, Perks[7] reported that corrosion of 20 of 24 specimens he studied initiated at

* Corresponding author
Email address: corr@hhu.ac.kr

voids along the rebar trace.

Steel surface conditions also affect corrosion processes of reinforcing steel in concrete. González et al.[8] reported that polished steel provided better chloride resistance than did rusted-steel. According to these authors, mortar alkalinity by itself or that of a $Ca(OH)_2$ saturated solution suffices to rapidly passivate a clean steel surface but does not ensure passivation of highly pre-rusted steel. Also, Li et al.[9] reported that sandblasting to remove mill scale and rust on the rebar surface was beneficial in increasing the chloride threshold in simulated pore solutions. To the contrary, Mehmood et al.[10] reported that the presence of a rust film on the rebar surface had an inhibiting effect on the onset of chloride induced corrosion in concrete.

Also, Hansson[11] found higher $[Cl^-]_{th}$ for rusted steel compared to steel with a clean or mill scale finish. Thus, the effects of steel surface on the corrosion initiation of reinforcing steel are conflicting.

The above studies aside, only limited research has been performed on the role of air voids in corrosion initiation. The purpose of the present experiments and analyses was to 1) characterize the steel-concrete interface of the G109 specimens in terms of air void size and distribution, 2) evaluate the tendency of corrosion initiation in terms of air void size and 3) evaluate any effect of steel surface condition on air void distribution at the interface.

## 2. Experimental procedures

### 2.1 Specimen fabrication and exposure

Cements of two alkalinities were employed in fabricating reinforced G109 type specimens. Table 1~2 lists the compositional analysis of cements with Equivalent Alkalinity (determined by $EqA = w/o\ Na_2O + 0.658\cdot w/o\ K_2O$) and mix design respectively EqA 0.32 and 1.08 were designated as low alkalinity (LA) and high alkalinity (HA), respectively. In addition, water cement ratio 0.50 was adapted for both types of specimens to ensure corrosion onset in a relative short time. The diameter of reinforcing steel was 12.7mm and surface conditions of reinforcement were 1) as-received surface (AR) and 2) polished surface (P) by wire brush. To measure macro-cell current between top and bottom bars, 100-Ohm resister mounted across them.

Fig. 1 schematically shows the geometry of standard G109 type specimen.[12] These specimens were exposed to normal laboratory environment with one-week wet and one-week dry ponding cycle. A 15 w/o NaCl solution was adapted as a ponding solution to minimize corrosion initiation time. Total 22 specimens were organized into four groups and four specimens were configured for each group except LA0.50 type specimens. For this type 10 specimens were configured to get a more statistical result. Table 3 lists the specimen configuration and components.
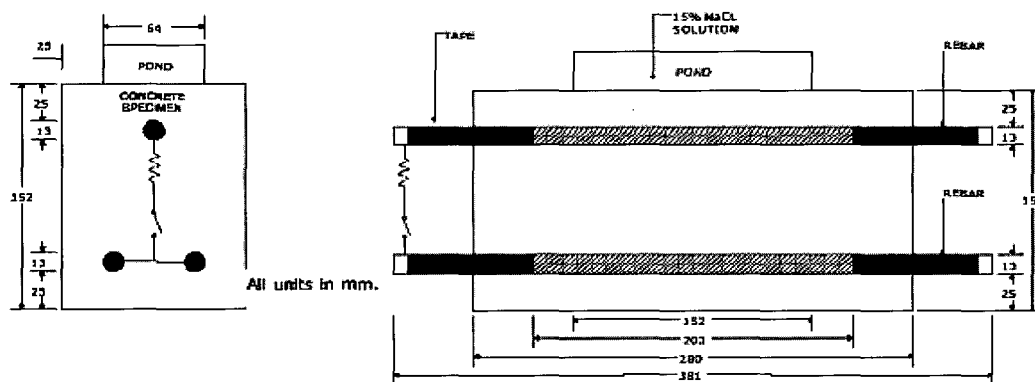


**Fig. 1** The geometry of classical G109 specimen

**Table 1** Compositions of LA and HA cement types

| Compound | $SiO_2$ | $Al_2O_3$ | $Fe_2O_3$ | $Fe_2O_3$ | MgO | $SO_3$ | $Na_2O$ | $K_2O$ | EqA |
|---|---|---|---|---|---|---|---|---|---|
| LA | 19.83 | 4.94 | 4.59 | 64.84 | 0.85 | 2.78 | 0.126 | 0.29 | 0.32 |
| HA | 20.40 | 5.33 · | 2.70 | 62.78 | 2.61 | 4.02 | 0.274 | 1.22 | 1.08 |

**Table 2** Specimen mix design

| Cement type | w/c | Cement(II) (kg/m³) | Water (kg/m³) | Sand (kg/m³) | Stone (kg/m³) | Fly ash (kg/m³) | WRDA 64 (kg/cwt) | WRDA-10 (kg/cwt) |
|---|---|---|---|---|---|---|---|---|
| LA | 0.37 | 388.4 | 143.5 | 742.9 | 980.1 | 0 | 0.17 | 0.57 |
| HA | 0.50 | 388.4 | 193.9 | 610.0 | 980.1 | 0 | 0.17 | 0 |

## 2.2 Measurements and analyses

Monitoring and data acquisition included potential and macro cell current measurement. In the early exposure, potential and macro-cell current were measured at every other day. Subsequently, the measuring period was extended up to one week. The potential criterion (negative than -280mV vs. Saturated Calomel Electrode)[13] was employed to define corrosion initiation. Once this occurred, specimens were autopsied and visually examined. The procedure included determination of the number and size of air voids along the top half of the upper steel surface. This size determination was based upon a diameter measurement assuming the voids to be half spheres or elliptical. That is, air voids (greater than 0.5mm in diameter) were counted by every 0.25mm increment and tabulated. Fig. 2 schematically described the way to decide air void size which does and does not have equal diameter. Table 4 shows typical example of void analysis for active site and whole area on the upper rebar trace where $V_a$ is void number at active site and $V_t$ is total void number along the whole rebar trace.

## 3. Results and discussion

### 3.1 Specimen dissection

When specimen became negative than -280mV$_{SCE}$, the
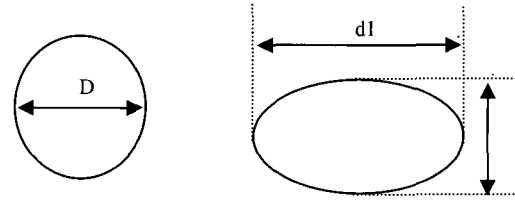


a) Half sphere (Dia = D)    b) Elliptical shape (Dia = [d1+d2]/2)

**Fig. 2** Typical example of air void size calculation

specimen was considered to be corroded and dissected for visual inspection. Fig. 3 shows a typical example of this for Specimen No. 7 (LA0.50-AR) and an air void (or voids) was found at corrosion initiation site. For most cases, visual observation of active specimens revealed one or more air voids at the active corrosion site. Based upon the observations, it is concluded that concrete voids may have facilitated passive film breakdown and onset of localized corrosion for the present specimens. If this was the case, then the mechanism probably involved a concentration cell with contiguous concrete coated and bare steel serving as cathodes and anodes, respectively. In this regard, it has previously been reported that such a cell has a relatively high driving potential and is likely to be compounded by an unfavorable surface area ratio (small anode versus large cathode).[14]

**Table 3** Listing of specimen configuration and major component

| Specimen No. | Specimen ID | w/c | Rebar Surface | Cement Alk. | Specimen No. | Specimen ID | w/c | Rebar Surface | Cement Alk. |
|---|---|---|---|---|---|---|---|---|---|
| 01~10 | LA0.50 | 0.50 | AR | Low (0.32) | 15~18 | HA0.50 | 0.50 | AR | High (1.08) |
| 11~14 | LA0.50-P | 0.50 | P | | 19~22 | HA0.50-P | 0.50 | P | |

**Table 4** Typical example of void analysis on the upper rebar trace (No. 17 HA0.50-AR)

*Void distribution on the upper rebar trace*
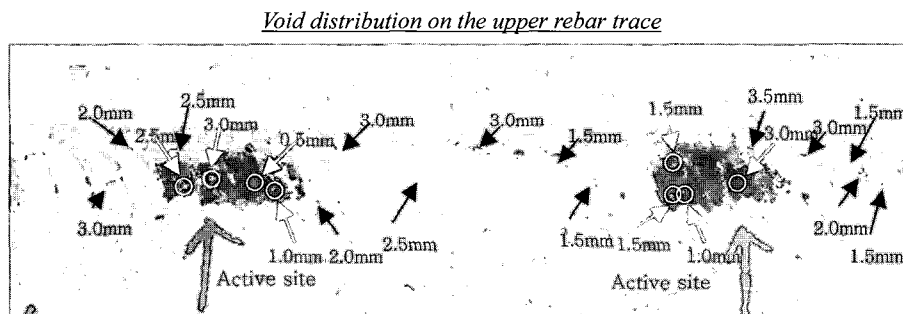


| Void number ($V_a$/ $V_t$) | | | | | | | |
|---|---|---|---|---|---|---|---|
| 0.50 | 1/30 | 0.75 mm | 0/20 | 1.00 mm | 0/14 | 1.25 mm | - |
| 1.50 | 2/6 | 1.75 mm | - | 2.00 mm | 0/3 | 2.25 mm | - |
| 2.50 | 1/3 | 2.75 mm | - | 3.00 mm | 2/6 | 3.25 mm | - |
| 3.50 | 0/1 | 3.75 mm | - | 4.00 mm | - | 4.25 mm | - |
| 4.50 | - | 4.75 mm | - | 5.00mm | - | > 5.0 mm | - |
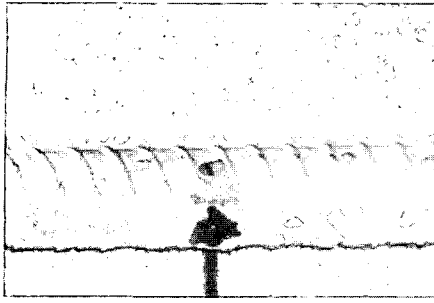
**Fig. 3** Typical example of an air void on corrosion initiation site (No. 7 LA0.50-AR)



**Fig. 4** Average cumulative number of voids along the rebar trace as a function of void diameter



**Fig. 5** Cumulative percent distribution of air voids at active sites and along the entire bar in terms of void size



**Fig. 6** The ratio of total void number at corrosion sites (VBBaBB) to the total number of voids along the whole upper rebar trace (VBBtBB) as a function of void diameter

## 3.2 Void distribution

Fig. 4 shows a plot of the average cumulative number of voids which were 0.50mm in diameter and larger as a function of void diameter. It is apparent from this plot that there was a greater number of voids for the HA compared to LA type specimens. Also, void size distribution was slightly irregularly allocated in case of HA type specimens compared to LA ones. According to Dubovoy et al.[15], high alkali contents in cement can cause an un-stable air-void systems; however, it is not clear whether this was a consequence of the nature of the materials or reflects inadvertent variations in different concrete batches. Also, specimens with the wire-brushed surface (P) had a lower number of voids than for the as-received condition for both cement alkalinities. This suggests that air voids preferentially formed on the rougher as-received surface rather than the smoother wire brushed one.

## 3.3 Effects of air void on corrosion onset

Fig. 5 presents a plot of, first, the average cumulative number of voids (percent basis) per specimen along the entire upper bar trace versus void diameter and, second, the average cumulative number of voids at the corrosion site (cumulative percent basis also) versus void diameter for the HA type specimens with as-received and wire brushed steel. This indicates that one or more voids were present at the corrosion initiation site for most of specimens. For both pairs of distributions, the active site ones initiate at and are displaced toward greater void diameter. This suggests that the tendency for corrosion initiation increased in proportion to void size irrespective of specimen type. This result is more clearly described in Fig. 6 which shows the ratio of void number at the corrosion site ($V_a$) to total number of voids ($V_t$) as a function of void size. Although the data are scattered, the chance of void participation on the corrosion onset increased in the proportion to void size, indicating that corrosion occurred preferentially at larger air voids.
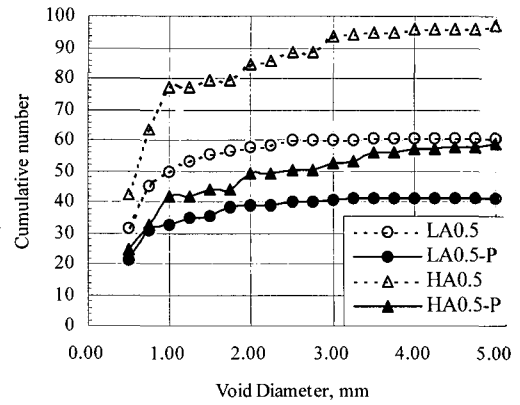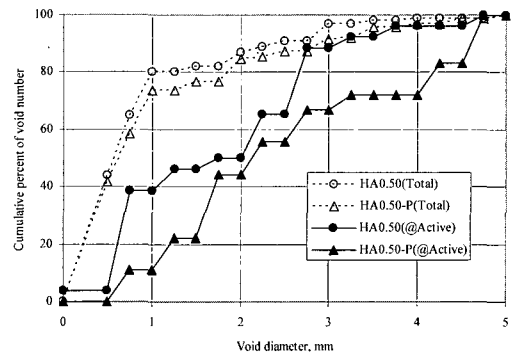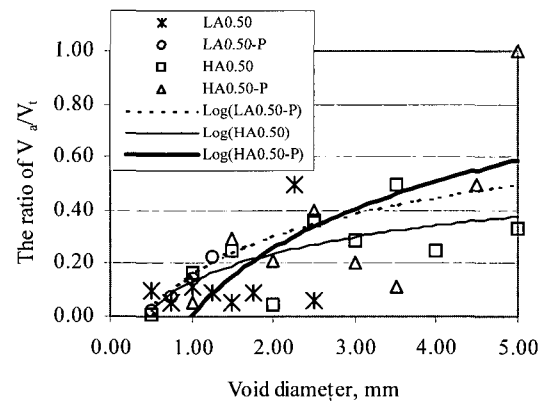
Concerning the role of air void on the corrosion initiation Mohammed et al.[16] reported chloride threshold values, [Cl⁻]th, in excess of two percent (w/o cement) when the concrete-steel interface was well compacted. Also, Glass and Reddy[6] reported that [Cl⁻]th was inversely proportional to the total area of air voids at the steel-concrete interface. Thus, possibly air voids at the interface provide inhomoge-
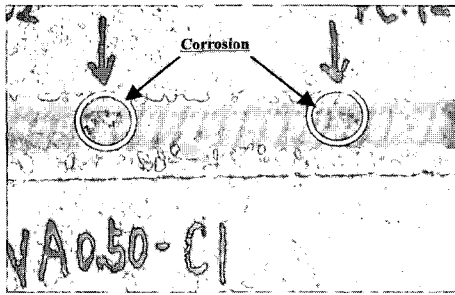
**Fig. 7** Photograph of corrosion on the as-received rebar embedded in low alkalinity type specimen (Specimen No. 5 LA0.50-AR)
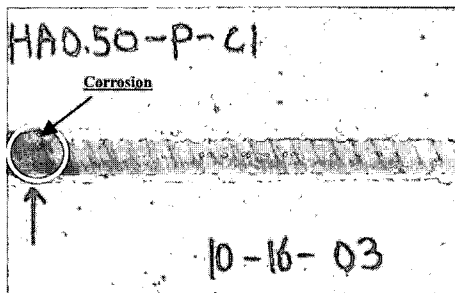


**Fig. 8** Photograph of corrosion on the polished rebar embedded in high alkalinity specimen(Specimen No.21 HA0.50-P)

neities along the rebar trace causing these sites preferentially to be anodic and provide space that holds pore water of diluted alkalinity lowering $[Cl^-]_{th}$ level compared to what is the case elsewhere. Presumably, the greater air void the more possibility of this trend.

### 3.4 Effects of steel surface on the corrosion features

For most cases, highly localized corrosion was found for wire brushed rebar specimens irrespective of cement alkalinity; however, the as-received rebars showed more broadly scattered general corrosion along the entire steel surface with some more advanced localized corrosion. Fig. 7 shows an example of the former and Fig. 8 shows the latter case.

These results indicate that the passive film was poorly formed on the as-received rebar. In this regard, González et al.[8] reported that a $Ca(OH)_2$ saturated solution rapidly passivated a clean steel surface but did not ensure passivation of highly pre-rusted steel. That is, in the case of wire brushed steel there was more abundant $[OH^-]$ compared to $[Fe^{n+}]$ which enabled formation of a relatively protective passive film compared to the as-received case. Also, less void formation for cleaned rebar surface can be another reason for the higher corrosion resistance of polished reabr.

## 4. Conclusion

The following conclusions were reached based upon the analysis of reinforced G109 concrete specimens that were subjected to cyclic wet-dry ponding with a 15 w/o NaCl solution:

1) Voids at the steel-concrete interface facilitated passive film breakdown and onset of localized corrosion. Based upon this, the initiation mechanism probably involved a concentration cell with contiguous concrete coated and bare steel serving as cathodes and anodes, respectively.

2) The corrosion tended to initiate at relatively large voids. Based upon voids being a factor in corrosion initiation, the possibility exists that durability of concrete structures can be enhanced by any treatment that reduces void size and density.

3) There was a greater density for voids to occur in the HA compared to LA type specimen. It is not clear whether this was a consequence of the nature of the different materials or reflects inadvertent variations in concrete batches. Also, specimens with wire-brushed steel (P) had a lower number of voids at the interface for both cement alkalinities, suggesting that air voids preferentially formed on the rough as-received surface compared to the smooth wire brushed one.

## References

1. D. A. Hausmann, "Steel Corrosion in Concrete- How Does It Occur?," *Material Protection*, Vol.6, 1967, pp.19~23

2. P. Sandberg, K. Pettersson, H.E. SØrensen, and H. Arup, Critical chloride concentrations for the onset of active reinforcement corrosion, RILEM, 1997, pp.453~459.

3. G. K. Glass and N. R. Buenfeld, Chloride threshold levels for corrosion induced deterioration of steel in Concrete, RILEM, 1997, pp.429~440.

4. T. Yonezawa, V. Ashworth and R. P. M. Procter, "Pore Solution Composition and Chloride Effects on the Corrosion of Steel in Concrete," *Corrosion Engineering*, Vol. 44, No.7, 1988, pp.489~499.

5. G. E. Monfore and G. J. Verbeck, "Corrosion of Prestressed Wire in Concrete," *ACI Journal*, Vol.32, 1960, pp.491~515.

6. G. K. Glass and B Reddy, *The Influence of the Steel Concrete Interface on the Risk of Chloride Induced Corrosion Initiation*, COST521 Workshop, Luxembourg, 2002.

7. Robert A. Perks, *Chloride Thresholds for Initiation of Corrosion of Steel Reinforcement in Concrete*, Master thesis, Ocean Engineering Department, Florida Atlantic University, 2000.

8. J.A González, E. Ramírez, A. Bautista, and S. Feliu, "The Behavior of Pre-Rusted Steel in Concrete," *Cement and Concrete Research*, Vol.26, 1996, pp.501~511.

9. L. Li, *Pitting Corrosion and Chloride Corrosion Threshold of Reinforced Steel in Alkaline Solutions*, University of South Florida, 2000, 3pp.

10. T. Mehmood, S. N. Absan, and Mohammad S. Al-Mughaidi, *Atmospheric Rusting of Rebars and Its Effect on Reinforced Concrete Corrosion*, CORROSION 1998, NACE International, Houston, 1998, Paper No. 00633.

11. M. Hansson and B. Sorensen, *Corrosion Rates of Steel in Concrete*, ASTM STP 1065, 1990, 3pp.

12. ASTM Standard Test Method G109-99, "Determining the Effect of Chemical Admixture on the Corrosion of Embedded Steel Reinforcement in Concrete Exposed to Chloride Environments," *Annual book of ASTM standard*, Vol.03.02, American Society for Testing and Materials, 100 Barr Harbor Drive, West Conshohocken, PA.

13. "Half-cell Potentials of Uncoated Reinforcing Steel in Concrete," ASTM C876-91, *Annual book of ASTM Standards*, 1991, ASTM International, 100 Barr Harbor Drive, West Conshohocken, PA 19428-2959 USA.

14. R.L. Miller, W.H. Hartt, and R.P. Brown, "Stray Current and Galvanic Corrosion of Reinforcing Steel in Concrete," *Materials Performance*, Vol.15, 1976, pp. 20~27.

15. V. S. Dubovoy, S. H. Gebler, and P. Klieger. "Cement-Alkalinity Levels as It Affects Air-Void Stability, Freeze-Thaw Resistance, and Deicer Scaling Resistance of Concrete," Research and Development Bulletin RD 128.

16. T.U. Mohammed, T. Fukute, T. Yamaji, and H. Hamada, *Long Term Durability of Concrete Made with Different Water Reducing Chemical Admixtures under Marine Environment*, Concrete for Extreme Conditions, London, 2002, 233pp.